

Cell Reports Methods, Volume 2

Supplemental information

Improved Sendai viral system

for reprogramming to naive pluripotency

Akira Kunitomi, Ryoko Hirohata, Vanessa Arreola, Mitsujiro Osawa, Tomoaki M. Kato, Masaki Nomura, Jitsutaro Kawaguchi, Hiroto Hara, Kohji Kusano, Yasuhiro Takashima, Kazutoshi Takahashi, Keiichi Fukuda, Naoko Takasu, and Shinya Yamanaka

Figure S1

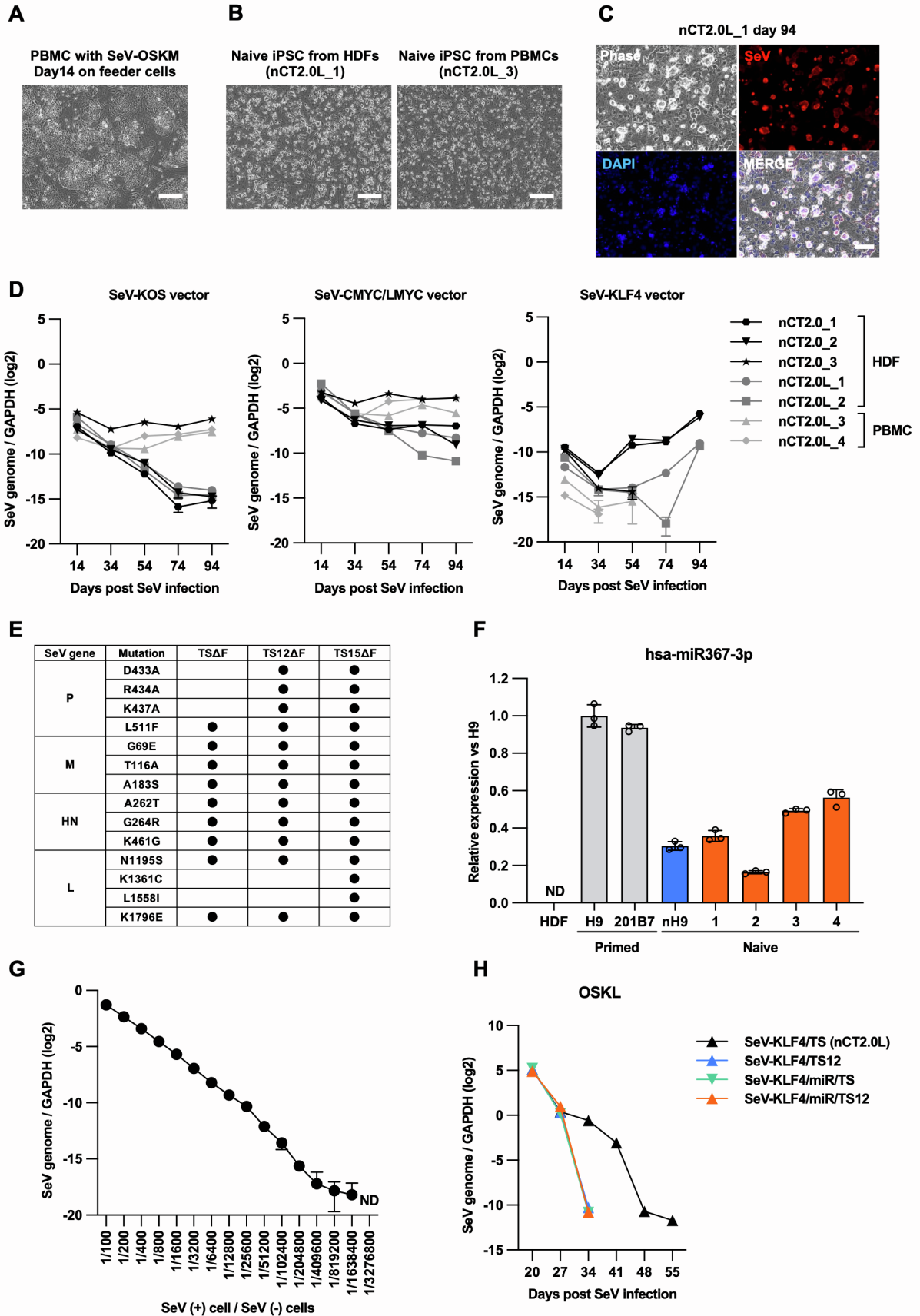


Figure S1 related to Figure 1. Characterization of conventional and modified SeV-KLF4 vectors.

(A) Representative phase-contrast image of PBMCs 14 days after CytoTune-iPS 2.0 SeV vector infection. Scale bar, 200 μm .

(B) Representative phase-contrast image of naive human iPSCs derived from HDFs (nCT2.0L_1) and PBMCs (nCT2.0L_3) reprogrammed with CytoTune-iPS 2.0L. Scale bar, 200 μm .

(C) Phase-contrast images of and immunofluorescent staining for SeV in naive human iPSCs (nCT2.0L_1) 94 days after SeV infection. Scale bar, 100 μm .

(D) qRT-PCR analysis of each SeV vector genome expression in naive human iPSCs reprogrammed with CytoTune2.0 or 2.0L normalized to the GAPDH expression. Data are shown as the mean \pm s.d. $n=3$ for each point.

(E) Point mutations of SeV genes in the SeV-TS Δ F, SeV-TS12 Δ F and SeV-TS15 Δ F vectors.

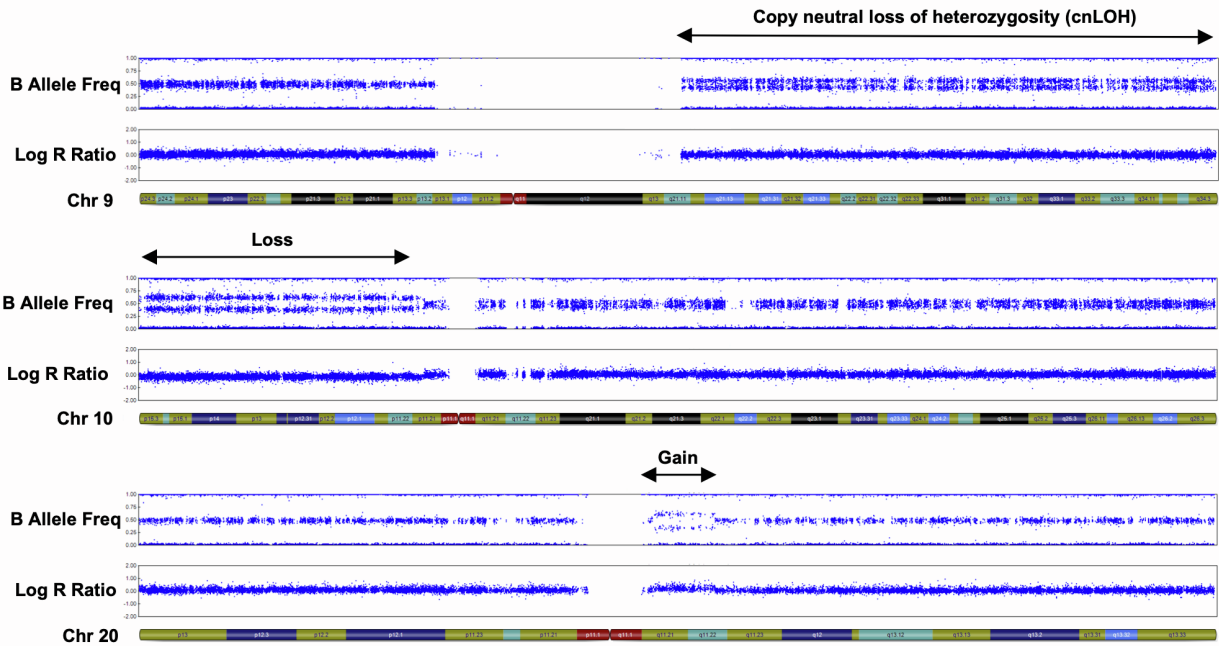
(F) qRT-PCR analysis of hsa-miRNA367-3p expression in HDFs and PSCs normalized to hsa-miRNA423-3p expression using TaqMan probes. Data are shown as the mean \pm s.d. $n=3$. ND, not detected even after 40 amplification cycles.

(G) Sensitivity of detection of the SeV genome in cells 14 days after SeV vector infection analyzed by qRT-PCR using TaqMan probes. The X-axis shows the rate of SeV-positive cells among SeV-negative cells.

(H) qRT-PCR analysis of SeV genome expression in primed iPSCs derived from HDFs by the co-infection of SeV-KOS and SeV-LMYC with SeV-KLF4 vectors using TaqMan probe. Data are shown as the mean \pm s.d. $n=3$ of each point.

Figure S2

A



B

No.	Type of CNV	Location	Size (bp)	nH9 (p109)	nOSKL_1 (p45)	nOSKL_2 (p29)	nOSKL_3 (p18)	nOSKL_4 (p16)	nOSKL_FF_1 (p21)	nOSKL_FF_2 (p21)
1	gain	chr1:51,440,093-51,804,731	364,639	-	○	-	-	-	○	-
2	loss	chr2:181,333,307-181,967,075	633,769	-	○	-	-	-	-	-
3	loss	chr3:60,305,117-60,518,998	213,882	○	-	-	-	-	-	-
4	cnLOH	chr3:60,542,151-60,597,001	54,851	-	-	-	-	-	○	-
5	cnLOH	chr5:58,428,799-58,620,440	191,642	-	○	-	-	-	-	-
6	loss	chr6:26,198,916-26,237,457	38,542	-	○	-	-	-	-	-
7	loss	chr6:162,392,902-162,914,986	522,085	-	○	-	-	-	-	-
8	cnLOH	chr9:68,167,130-141,066,491	72,899,362	○	-	-	-	-	-	-
9	cnLOH	chr9:71,100,140-141,066,491	69,966,352	-	-	-	-	-	○	○
10	loss	chr10:98,087-23,539,203	23,441,117	-	-	○	-	-	-	-
11	loss	chr10:43,530,071-68,593,991	25,063,921	-	○	-	-	-	-	-
12	loss	chr10:68,259,319-68,461,866	202,548	-	-	-	-	-	-	○
13	loss	chr10:98,087-35,901,715	35,803,629	○	-	-	-	-	-	-
14	cnLOH	chr11:125,276,400-125,881,102	604,703	-	○	-	-	-	-	-
15	gain	chr12:191,619-14,939,009	14,747,391	-	○	-	-	-	-	-
16	gain	chr13:42,151,623-42,465,713	314,091	-	○	-	-	-	-	-
17	cnLOH	chr15:22,576,118-87,876,646	65,300,529	○	-	-	-	-	-	-
18	cnLOH	chr15:22,784,095-102,369,711	79,585,617	-	-	-	-	○	-	-
19	gain	chr18:6,873,354-7,688,505	815,152	-	○	-	-	-	-	-
20	gain	chr18:6,912,332-6,951,060	38,729	-	○	-	-	-	-	-
21	cnLOH	chr19:260,912-59,097,160	58,836,249	-	-	-	-	○	-	-
22	gain	chr20:30,183,598-33,720,033	3,536,436	○	-	-	-	-	-	-
23	cnLOH	chr22:43,767,079-51,195,728	7,428,650	○	-	-	-	-	-	-
24	cnLOH	chrX:2,715,425-58,339,545	55,624,121	-	○	-	-	-	-	-
25	loss	chrX:2,760,060-155,123,035	152,362,976	○	-	-	-	-	-	-
26	loss	chrX:32,003,841-32,116,068	112,228	-	○	-	-	-	-	○
27	cnLOH	chrX:62,058,620-154,916,845	92,858,226	-	○	-	-	-	-	-

Figure S2 related to Figure 2. SNP genotyping array results of naive PSCs in this study.

- (A) Representative CNVs found in nH9 ESC: copy neutral loss of heterozygosity (cnLOH) in Chr 9, loss in Chr 10, gain in Chr 20.
- (B) All CNVs detected in the naive PSCs after reprogramming.